

Multiple phases in sputtered Cr₂CoGa films

Manuel P. Geisler, Markus Meinert, Jan Schmalhorst, Günter Reiss

Center for Spinelectronic Materials and Devices, Department of Physics, Bielefeld University, D-33501 Bielefeld, Germany

Elke Arenholz

Advanced Light Source, Lawrence Berkeley National Laboratory, CA 94720, USA

Abstract

By magnetron co-sputtering, thin films of a nominal Cr₂CoGa compound were deposited on MgO and MgAl₂O₄. To achieve crystallisation in the inverse Heusler structure, different heat treatments were tested. Instead of the inverse Heusler structure, we observed phase separation and precipitate formation in dependence on the heat treatment. The main precipitate is Cr₃Ga in A15 structure. The remainder forms Co-rich CoGa in the B2 structure and possibly Cr-rich CoCr in the σ -phase.

1. Introduction

Theoretical work on Cr₂CoGa in inverse Heusler structure predicts it to be a nearly fully compensated half-metallic ferromagnet as a consequence of the Slater-Pauling rule [1]. Further calculations indicate a Curie temperature of 1520 K [2], which would be the largest among known Heusler compounds [3]. Such a material has the potential to be an ideal electrode for spin torque devices [4]. Experimentally, several attempts to synthesise Cr₂CoGa in bulk were already performed. According to them, the compound crystallizes in a cubic structure, which could be the inverse Heusler structure X_a [5, 6]. This structure has an fcc lattice with a four atom basis at the internal coordinates A = (0, 0, 0), B = ($\frac{1}{4}$, $\frac{1}{4}$, $\frac{1}{4}$), C = ($\frac{1}{2}$, $\frac{1}{2}$, $\frac{1}{2}$) and D = ($\frac{3}{4}$, $\frac{3}{4}$, $\frac{3}{4}$). The four atoms of a compound X₂YZ have the occupation sequence Y – X – X – Z such that inversion symmetry is not present. This structure belongs to space group $F\bar{4}3m$ (No. 216). However, the system appears to be highly susceptible for atomic disorder and a much lower Curie temperature of about 300 K was found [7].

In order to explain this discrepancy, a stability analysis of Cr₂CoGa in X_a structure was performed in a previous work [8]. It was found that the inverse Heusler phase of this compound is unstable with respect to both constituent elements, binary and ternary decompositions. This instability is indicated by the slightly positive formation energy $\Delta E_0^{\text{Cr}_2\text{CoGa}} = 0.08$ eV/f.u. and negative formation energies for binary phases. The formation of multiple phases is consequently energetically more preferable than the single ternary phase. However, the formation energy of the X_a phase is rather close to zero and it is known that calculated formation energies may differ from actual formation enthalpies at typical synthesis temperatures [9, 10]. These differences are typically of the order 0.1 eV/atom which may enable the exis-

tence of Cr₂CoGa in inverse Heusler structure as a metastable phase.

In this work we investigate nominal Cr₂CoGa thin films synthesised via magnetron co-sputtering on single crystal substrates with the aim to enforce the crystallization by epitaxial constraints.

2. Methods

Films of 20 nm thickness were deposited in a magnetron co-sputtering device. Elemental targets with at least 99.99% purity were used. After deposition, all thin films were covered with 2 nm of MgO via electron beam evaporation. X-ray fluorescence was used to adjust the film stoichiometry. MgO and MgAl₂O₄ (MAO) with [001] cut were tested as substrates with deposition temperatures up to 700°C and cooling rates below 30 K/min. Calculations predict a lattice constant of 5.78 Å for Cr₂CoGa [8], so that lattice mismatches of –2.9 % (MgO) and +1.0 % (MgAl₂O₄) are expected when the usual 45° rotation of the unit cells is taken into account.

Further sample characterization methods were x-ray diffraction (XRD) and reflectivity (XRR), scanning electron microscope (SEM) imaging and energy dispersive x-ray (EDX) mappings. XRD and XRR measurements were performed with a Philips X'Pert Pro diffractometer with a Cu anode, Bragg-Brentano and point-focus collimator optics. Additionally, a Euler cradle was used to search for superstructure reflections. The device used for SEM imaging and EDX mappings is a FEI Helios Nanolab 600 with an EDAX Apollo detector.

Measurements of magnetic circular dichroism (XMCD) and specific x-ray absorption (XAS) were performed at the Advanced Light Source, Berkeley, beamline 6.3.1. The absorption signal was determined in total electron yield and transmission with a photodiode monitoring the substrate luminescence [11]. A magnetic field of ± 1.8 T was applied and the spectra were taken at 80 K.

Email address: meinert@physik.uni-bielefeld.de (Markus Meinert)

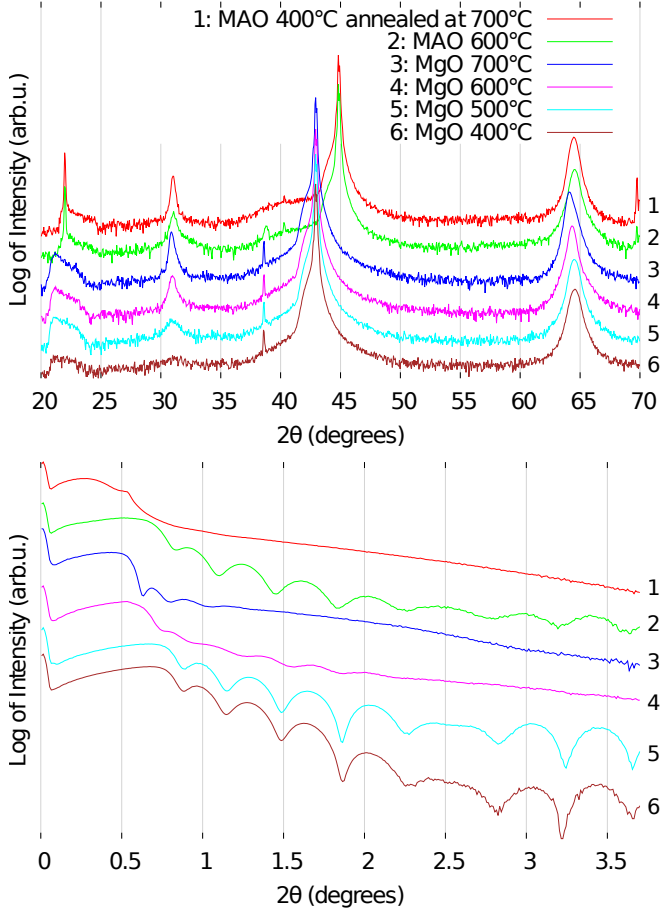


Figure 1: XRD (top) and XRR (bottom) measurements of six different Cr_2CoGa samples. All sharp peaks and broad peaks below $2\theta = 25^\circ$ originate from the substrates.

Phase decompositions were studied theoretically using the data from the *Materials Project* database [12, 13]. The formation energy of Cr_2CoGa was computed with the ELK full-potential linearised augmented-plane wave (FP-LAPW) code [14]. Both the *Materials Project* and our total energy calculations are based on the Perdew-Burke-Ernzerhof (PBE) functional [15]. Crystal structure visualizations were generated with VESTA [16].

3. Results

Figure 1 shows results of XRD and XRR measurements of six different samples deposited under various conditions. The XRR spectra indicate that the films get rough at deposition or annealing temperatures of 600°C and more. The main diffraction peaks at 30.9° and 64.4° have distinct deposition temperature dependences. While the latter reflection varies not too much, the first reflection gets more intense and narrower with increasing deposition temperature. Assuming the observed main reflections belong to the X_a phase, we define the order parameter

$$S = \sqrt{\frac{I_{(002)}^{\text{exp.}}/I_{(004)}^{\text{exp.}}}{I_{(002)}^{\text{theo.}}/I_{(004)}^{\text{theo.}}}}, \quad (1)$$

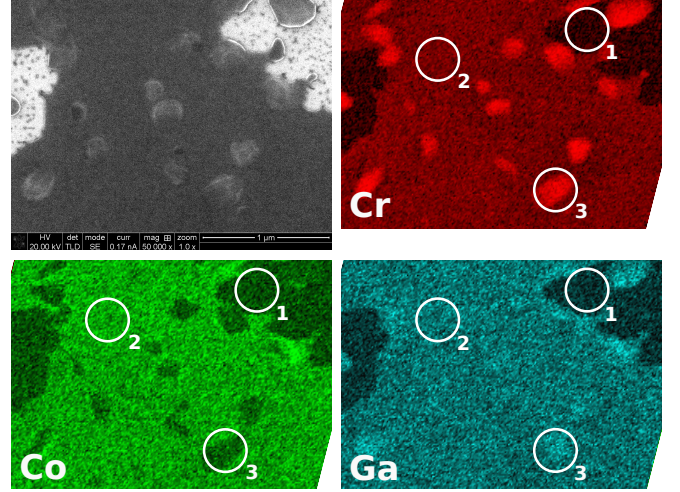


Figure 2: SEM and EDX mapping images of a nominal Cr_2CoGa sample on MAO deposited at 600°C .

which is sensitive to disorder between A/B sites, A/D sites, and C/D sites, whereas it is insensitive to disorder between A/C sites, B/D, and B/C sites. In the case of Heusler compounds, it is equivalent to S_{B_2} [17] and is related to the number of X atoms on Y or Z sites. With the above definition we found $S_1 = 1.07$, $S_2 = 1.21$, $S_3 = 1.11$ and $S_4 = 1.04$, where the subscript numbers refer to the numbers in Figure 1. For A/B disorder or strong C/D disorder we can have $1 < S < 1.092$. In both cases, the structure changes to the regular Heusler type, which is however energetically highly unfavorable ($+0.65$ eV/f.u. with respect to the inverse type [2]). Further, the large S_2 cannot be explained this way. Therefore we conclude that the two peaks do not originate from the X_a phase nor from the regular Heusler phase. For traces 5 and 6 we have $S_{5,6} \ll 1$, so a possible superstructure is only weakly present. At high deposition temperatures, a broad reflection around $2\theta = 39^\circ$ is observed, particularly on MAO. We have searched for the (111) or $(11\bar{1})$ superstructure reflections of a possible inverse Heusler phase to which the two main reflections may belong by pole figure scans around $2\theta = 26.7^\circ$. The reflections could not be observed, which excludes the formation of the Heusler or inverse Heusler structure.

To investigate the deposition temperature dependent film roughness, SEM images and EDX mappings were taken. Figure 2 shows the images taken on a sample deposited at 600°C on MAO. As indicated, the mapping reveals the existence of three rather different regions of the sample. Region 1 and areas similar to it do not show a film, giving rise to the charging in the SEM image. Most parts of the mapped area look like region 2, where all sputtered elements can be found. Region 3 is an example of grains of Cr and Ga, which are essentially free of Co. Other samples look quite similar to the sample shown here.

Figure 3 exemplarily shows the results of XMCD measurements of a sample deposited at 600°C on MgO. The weak XMCD signal points to either essentially nonmagnetic Cr and Co, or to nearly compensated ferrimagnetism for each element individually. The shoulders visible in the Cr XAS can be attributed to oxidation; they are more pronounced in rougher

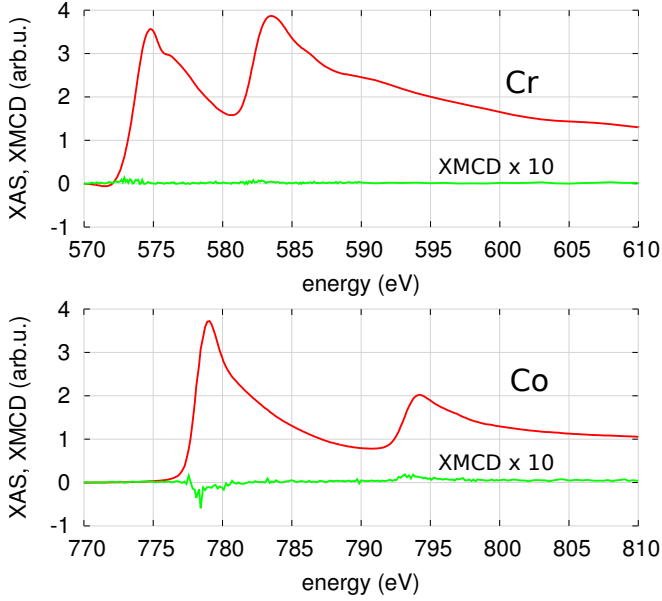


Figure 3: XAS and XMCD spectra on Cr and Co $L_{3,2}$ edges of a nominal Cr_2CoGa sample deposited at 600°C on MgO. The spectra were taken in total electron yield at 80 K.

samples, where the protective MgO layer is not thick enough to prevent the oxidation. The very weak XMCD is present both in surface sensitive electron yield spectra and in the bulk sensitive transmission spectra. The Co XAS is nearly free of additional structures, in contrast to typical XAS line shapes of Co in Heusler and inverse Heusler compounds [18, 19]. All samples that we have investigated had similarly weak XMCD signals.

Taking together the experimental findings, we attempt to identify the phases into which the Cr_2CoGa films separate with guidance from the computed formation energies in Table 1, the binary phase diagrams [20, 21, 22] and the high-temperature ternary phase diagrams of Co-Cr-Ga [23]. The Co-poor precipitates are most likely binary Cr-Ga compounds. In the Cr-Ga system four intermetallic phases are known, of which CrGa decomposes below 736°C . The three stable phases are Cr_3Ga with A15 structure (space group $Pm\bar{3}n$, cf. Fig 4 b)), CrGa_4 with PtHg_4 structure (space group $Im\bar{3}m$) and Cr_5Ga_6 with unknown structure. All these phases are either para- or diamagnetic. According to the EDX mapping, the precipitates are rich in Cr, so it is likely that they are mainly Cr_3Ga . The broad reflection observed in the XRD spectra around $2\theta = 39^\circ$ can be explained as the (002) reflection of this phase with $a \approx 4.6 \text{ \AA}$. In view of the broad reflection, these precipitates have to be polycrystalline with a crystallite size around 2 nm. The formation of this phase is also very likely in terms of the formation energy, see Table 1; the remainder of the film could crystallize as Co_2CrGa in the regular Heusler structure, which is known to exist [23], and is seemingly energetically favorable. This could account for the main x-ray reflections around $2\theta \approx 31^\circ$ and $2\theta \approx 64^\circ$, but the corresponding (111) reflection around $2\theta = 26.7^\circ$ was not observed. Assuming a B2-type (cf. Figure 4 c)) disordered phase like $\text{Co}(\text{Ga}_x\text{Cr}_{1-x})$ with $x = 0.5$, which is energetically less favorable, would explain

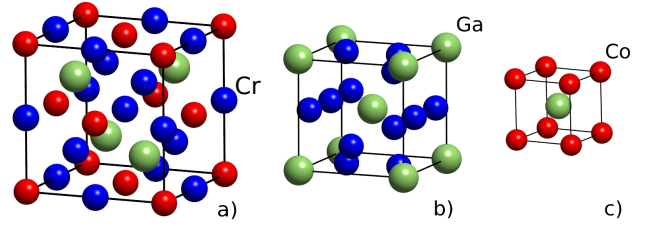


Figure 4: a): Ideal inverse Heusler structure of Cr_2CoGa . b): Cr_3Ga in A15 structure. c): CoGa in B2 structure.

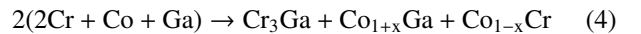
the missing (111) reflection. However, it is also calculated to be a ferromagnet with $1.67\mu_B$ on Cr and $0.64\mu_B$ on Co, at odds with the XMCD results. Thus, we assume that either the deposition temperature was insufficient to form Co_2CrGa or it decomposes during the slow cooling. It is known that various phases occur in the Co-Cr-Ga system near the Co_2CrGa composition below 800°C , namely hcp-Co, B2 CoGa, and $D8_b$ CoCr (also known as σ -CoCr) [23]. Only at temperatures higher than our deposition temperature, significant amounts of Cr will dissolve in B2 CoGa. Thus, CoGa with $a = 2.88 \text{ \AA}$ and a strong (001) texture due to the epitaxial matching with the substrate is the best candidate to explain the observed XRD spectra. The two main peaks can be indexed as the (001) and (002) reflections of this phase and no reflections below $2\theta = 31^\circ$ would be present. This compound is paramagnetic and becomes weakly ferromagnetic at increased Co content [24]. The Co-rich B2 phase is stable up to about 63at.% Co at our deposition or annealing conditions. At this composition, a Curie temperature around 350 K and a magnetization of $0.8\mu_B$ per unit cell may be expected from extrapolation of solid-solution experiments:

$$T_C = 2.33x^2 \text{ K}/(\text{at.}\%)^2, \quad (2)$$

$$m = 0.31x^2 \text{ emu/g}/(\text{at.}\%)^2, \quad (3)$$

with x being the excess amount of Co ($50 + x$) given in at.% [24]. Quenching from high temperature would freeze this state and the above values are in agreement with earlier experiments on quenched bulk material [5, 7]. In our case, the magnetic moment of Co at 80 K is virtually zero, so that this extrapolation allows us to conclude that there is less than 6% excess Co, as one expects from the binary phase diagram for slowly cooled CoGa [20]. The expected (001)/(002) peak intensity ratio matches the observed values when about 15% disorder between Co and Ga sites is taken into account. More disorder strongly diminishes the (001) reflection as in traces 5 and 6 of Figure 1, which represent samples with lower deposition temperatures.

The remainder of the material could form a Cr-rich σ -phase [23], which would be weakly magnetic [25]. If these crystallites remained sufficiently small, they could not be detected in the EDX mapping or with XRD. The reaction



is thus our final conjecture for the decomposition of nominal Cr_2CoGa , which explains the XRD, EDX mapping, and element specific magnetization data of our films.

reaction	ΔE_0 (eV/f.u.)
a) $2(2\text{Cr} + \text{Co} + \text{Ga}) \rightarrow \text{Co}_2\text{CrGa} + \text{Cr}_3\text{Ga}$	-0.61
b) $2\text{Cr} + \text{Co} + \text{Ga} \rightarrow \text{GaCo} + 2\text{Cr}$	-0.56
c) $2(2\text{Cr} + \text{Co} + \text{Ga}) \rightarrow \text{Cr}_3\text{Ga} + \text{GaCo} + \text{Co} + \text{Cr}$	-0.38
d) $3(2\text{Cr} + \text{Co} + \text{Ga}) \rightarrow \text{Ga}_3\text{Co} + 6\text{Cr} + 2\text{Co}$	-0.35
e) $2(2\text{Cr} + \text{Co} + \text{Ga}) \rightarrow 2\text{Co}(\text{Ga}_{0.5}\text{Cr}_{0.5}) + \text{Cr}_3\text{Ga}$	-0.18
f) $2\text{Cr} + \text{Co} + \text{Ga} \rightarrow \text{Cr}_2\text{CoGa}$	0.08

Table 1: Most favorable reactions forming binary and ternary phases and their reaction energies according to the *Materials Project* database for Cr_2CoGa .

4. Conclusions

We were able to show experimentally that Cr_2CoGa thin films deposited via magnetron sputtering do not form the desired half-metallic and ferrimagnetic X_a structure. Instead we find a segregation into CoGa with B2 and Cr_3Ga with A15 structure. Possibly also the σ -phase of CoCr is formed. The instability of the Cr_2CoGa compound makes this material unsuitable for the proposed applications in spintronics.

Acknowledgments

This work was supported by the European Commission via the Collaborative Project HAFIR (Project No. 604398). Further financial support by the Deutsche Forschungsgemeinschaft (DFG) is gratefully acknowledged. We thank Dr. Karsten Rott for help with EDX mappings and SEM images. The Advanced Light Source is supported by the Director, Office of Science, Office of Basic Energy Sciences, of the U.S. Department of Energy under Contract No. DE-AC02-05CH11231.

References

References

- [1] S. Skaftouros, K. Ozdogan, E. Sasioglu and I. Galanakis, *Phys. Rev. B* 87 (2013) 024420.
- [2] I. Galanakis and E. Sasioglu, *Appl. Phys. Lett.* 99 (2011) 052509.
- [3] J. Kübler, G. H. Fecher and C. Felser, *Phys. Rev. B* 76 (2007) 024414.
- [4] T. Graf, C. Felser, and S. S. P. Parkin, *Prog. Solid St. Chem.* 39 (2011), 1-50.
- [5] M. Hakimi, M. Venkatesan, K. Rode, K. Ackland and J.M.D. Coey, *J. Appl. Phys.* 113 (2013) 17B101.
- [6] T. Graf, F. Casper, J. Winterlik, B. Balke, G.H. Fecher, and C. Felser, *Z. Anorg. Allg. Chem.* 635 (2009) 976.
- [7] J. F. Qian, L. Feng, W. Zhu, E. K. Liu, X. D. Tang, W. H. Wang, G. H. Wu, F. B. Meng, H. Y. Liu, H. Z. Luo, *Acta Physica Sinica* 60 (2011) 056402.
- [8] M. Meinert and M. Geisler, *J. Magn. Mater.* 341 (2013) 72.
- [9] M. Yin, S. Chen, and P. Nash, *J. All. Comp.* 577 (2013) 49-56.
- [10] B. Grabowski, L. Ismer, T. Hickel, and J. Neugebauer, *Phys. Rev. B* 79 (2009) 134106.
- [11] M. Kallmayer, H. Schneider, G. Jakob, H. J. Elmers, B. Balke, and S. Cramm, *J. Phys. D: Appl. Phys.* 40 (2007) 1552.
- [12] A. Jain, G. Hautier, C. Moore, S. P. Ong, C. Fischer, T. Mueller, K. Persson, and G. Ceder, *Com. Mat. Sci.* 50 (2011) 2295.
- [13] S. P. Ong, A. Jain, G. Hautier, M. Kocher, S. Cholia, D. Gunter, D. Bailey, D. Skinner, K. Persson, and G. Ceder, <http://materialsproject.org/>
- [14] <http://elk.sourceforge.net>, Version 1.4.22
- [15] J. P. Perdew, K. Burke, and M. Ernzerhof, *Phys. Rev. Lett.* 77 (1996) 3865.
- [16] K. Momma and F. Izumi, *J. Appl. Crystallogr.* 44 (2011) 1272.
- [17] Y. Takamura, R. Nakane, and S. Sugahara, *J. Appl. Phys.* 105 (2009) 07B109.

- [18] N. D. Telling, P. S. Keatley, G. van der Laan, R. J. Hicken, E. Arenholz, Y. Sakuraba, M. Oogane, Y. Ando, K. Takanashi, A. Sakuma, and T. Miyazaki, *Phys. Rev. B* 78 (2008) 184438.
- [19] M. Meinert, J.-M. Schmalhorst, C. Klewe, G. Reiss, E. Arenholz, T. Böhnert, and K. Nielsch, *Phys. Rev. B* 84 (2011) 132405.
- [20] H. Okamoto, *J Phase Equilib. Diff.* 26 (2005) 197.
- [21] H. Okamoto, *J Phase Equilib. Diff.* 28 (2007) 301.
- [22] K. Ishida and T. Nishizawa, *Bull. Alloy Phase Diagr.* 11 (1990) 357.
- [23] K. Kobayashi, R. Kainuma, K. Fukamichi, K. Ishida, *J. Alloy Compd.* 403 (2005) 161.
- [24] J. G. Booth and J. D. Marshall, *Phys. Lett.* 32A (1970) 149.
- [25] J. Pavlů, J. Vřešťál, and M. Šob, *Intermetallics* 18 (2010) 212.